PERGAMON

International Journal of Multiphase Flow 27 (2001) 1517–1532

International Journal of Multiphase Flow

www.elsevier.com/locate/ijmulflow

Measurement of fluid turbulence along the path of a heavy particle in a backward-facing step flow

D. McAndrew, S. Coppen, C.B. Rogers *

Mechanical Engineering Department, Tufts University, Medford, MA 02155, USA

Received 22 December 1999; received in revised form 13 February 2001

Abstract

To accurately model the motion of a solid particle in a turbulent air flow, characteristics of the fluid turbulence in the particle-Lagrangian reference frame must be known. This paper describes a quasi-numerical technique that uses a laser Doppler anemometer (LDA) probe mounted on a two-dimensional traverse to track the path of an emulated particle through a turbulent backward-facing step flow. Fluid velocity measurements (from the LDA) are inputs to a control loop that accelerates the LDA probe as if it were a particle allowing for particle-Lagrangian fluid statistics to be measured. Particles with time constants from 0.1 to 10 s were run through a backward-facing step flow with Reynolds number 10,000 based on step height and inlet velocity. Digital particle image velocimetry (DPIV) was used to estimate the fluid vorticity along the particle path. The results show that the particle behavior is a strong function of particle path. Particles entering the shear layer see a larger range of turbulence and therefore are more affected by the flow than those that stay outside the shear layer.

Keywords: Particle-laden flow; Two-phase flow; Particle–turbulence interaction; Laser doppler anemometer; Digital particle image velocimetry; Backward-facing step flow

1. Introduction

Dilute particle-laden flows occur throughout industry and in nature. From volcanic eruptions to combustion, the motion of a dilute second phase is dictated by both the weight of the particle and by the turbulence encountered by the particle along its path. The fact that the turbulence viewed by the particle is a function of the particle itself, further complicates modeling. Modeling began with the work of Tchen (1947), who presented a transport equation for a particle moving in

* Corresponding author. Fax: +1-617-627-3058.
E-mail address: crogers@tufts.edu (C.B. Rogers).

0301-9322/01/$ - see front matter
PII: S0301-9322(01)00019-2

a fluid. This equation has seen a number of modifications, with its most recent form being presented by Maxey and Riley (1983). The difficulty with these transport equations is that they require the knowledge of the fluid turbulence along the path of the particle. Yudine (1959) noted that gravitational drift would affect this path by pulling particles through turbulent neighborhoods, reducing the effect of the turbulence on the particle motion (''crossing trajectories'' effect). Snyder and Lumley (1971) demonstrated this through measuring the particle velocity autocorrelation for a number of different particles in a near-isotropic turbulent airflow, although they were unable to measure the fluid statistics in the reference frame of the moving particle.

Since the particle weight and ability of the particle to respond to the fluid velocity fluctuations (as measured by the particle response time or time constant) dictate this path, modelers must develop a method of mapping the turbulence into the moving reference frame of the particle (particle-Lagrangian). Current modelers have taken two different approaches: continuum modeling and particle tracking. Continuum models (e.g., Simonin et al., 1993) model the particle phase as a rarified gas. Particle-tracking algorithms (e.g., Berlemont et al., 1990) estimate local fluid velocities from the modeled turbulence energies and then move individual particles through the simulated flow field. Each approach has advantages and disadvantages, but both are hindered by a lack of experimental data for verification. Direct numerical simulations (for example, Squires and Eaton, 1991a,b; Elghobashi and Truesdell, 1992; Coppen et al., 1999) have the advantage that they can give almost all the information about the flow desired. The disadvantage is that the turbulence is rather simple (isotropic turbulence) and/or low Reynolds number (as is the case with the channel flow simulations of Rouson et al., 1997). Although the library of experimental data has rapidly increased in the past few decades (for example, Wells and Stock, 1983; Ruck and Makiola, 1988; Rogers and Eaton, 1990; Longmire and Eaton, 1992; Kiger and Lasheras, 1997), most of the experimental work can only measure properties or the fluid and the particle phases from a stationary Eulerian frame. Since particles will not sample all of the turbulence uniformly, the average fluid turbulence statistics measured in the Eulerian reference frame will differ substantially from those measured in the particle-Lagrangian one. The particles do not uniformly sample the turbulence because the turbulence can dictate their path. Areas of high vorticity can throw particles into regions of high strain, preferentially concentrating the particles (Eaton and Fessler, 1994). Coppen et al. (2001) has shown that this behavior falls over a large range of particles: from particles with response times on the order of one-tenth the fluid time scales to ten times the fluid time scales. Thus preferentially concentrated particles will tend to see a turbulence with lower vorticity than measurements taken at an Eulerian point.

In order to better understand how to make this transformation from the Eulerian to particle-Lagrangian reference frames, we developed an experimental technique that combines both numerical and experimental techniques to make measurements in the particle-Lagrangian reference frame. The idea is to actively move a two-component laser Doppler anemometer (LDA) along the path of a particle through a water flow. The LDA takes a single measurement of the flow, a computer calculates the local acceleration of a particle of given mass and response time if it were at that location in the flow and then accelerates the LDA at that rate. Therefore the LDA measuring volume will move through the flow, as though it were a particle. This technique, dubbed quasi-numerical simulation (QNS), is therefore essentially a numerical simulation with the water flow acting as a Navier–Stokes solver. The QNS was initially developed for a channel flow (Ainley et al., 1997), and this paper looks at particle motions in a backward-facing step. We

choose a backward-facing step flow because it can be simulated (Le et al., 1997) and has been exhaustively studied experimentally (e.g., Armaly et al., 1983; Ruck and Makiola, 1988). It has the advantage over the channel flow in that it gives some insight into particle motions in an inhomogeneous flow field.

For the QNS method to work, we have to assume that the particles do not affect the fluid phase, since there is no real particle in our flow. Further, to simplify the hardware, we constrain the emulated particle to move in two dimensions. Finally, to simplify the transport equation, we also assume that the emulated particle density is substantially higher than the density of the carrier fluid and that the gravitational drift of the particle is small so that we can use a simple linear Stokes drag law

$$\frac{\mathrm{d}V_\mathrm{p}}{\mathrm{d}t} = \frac{1}{\tau_\mathrm{p}}(U_\mathrm{f} - V_\mathrm{p}) - g, \tag{1}$$

where U_f is the local Eulerian fluid velocity and V_p is the local Eulerian particle velocity, (τ_p is the particle response time or time constant, and g is the gravitational acceleration). The experiment itself, however, uses water to simulate the air turbulence since the time scales are substantially slower than the corresponding ones in air. If the flow is isothermal, the turbulence should be the same in the two flows for identical Reynolds numbers. The experiment is further limited to particle motion in two dimensions.

2. Experimental setup

A backward-facing step flow was used in this experiment to further the investigation of particle–turbulence interaction. Previously, particle data were taken in a fully developed, turbulent channel flow and dispersion was found to increase with decreasing Stokes number (Ainley, 1997). With the backward-facing step channel, shear layer interaction can be investigated and compared to channel data.

Our system is composed of two distinct setups: the hardware that creates the backward-facing step flow and the hardware that controls the motion of the simulated particle (the LDA measuring volume). Fig. 1 shows a schematic of the backward-facing step and the traverse system. The LDA is mounted on a two-degree of freedom traverse that is capable of accelerating the probe at rates much higher than the fluid fluctuations in the turbulence. The recirculating water flows in a combination of Plexiglass and PVC piping. The test section itself is 5 cm high (one step height) and 15 cm wide (three step heights) upstream of the step and 10 cm by 15 cm downstream of the step. The 15 cm width was limited by the focal length of the LDA system. The LDA focal length, in turn, was dictated by the measuring volume size (0.4 mm), which had to be smaller than the fluid Kolmogorov length scale. Since this width is on the same order as the height, our step is not a purely two-dimensional flow. Finally, the channel was 48 step heights long (36 step heights after the step). The water is pushed through the test section with a 1.5 hp submersible motor with a 6 in. propeller. The fluid velocity measurements were taken with a TSI fiber probe system using an IFA 750 Burst Analyzer. The motion of the LDA was controlled by two Parker amplifiers and brushless DC servo motors with encoder feedback. These amplifiers were fed a velocity from the

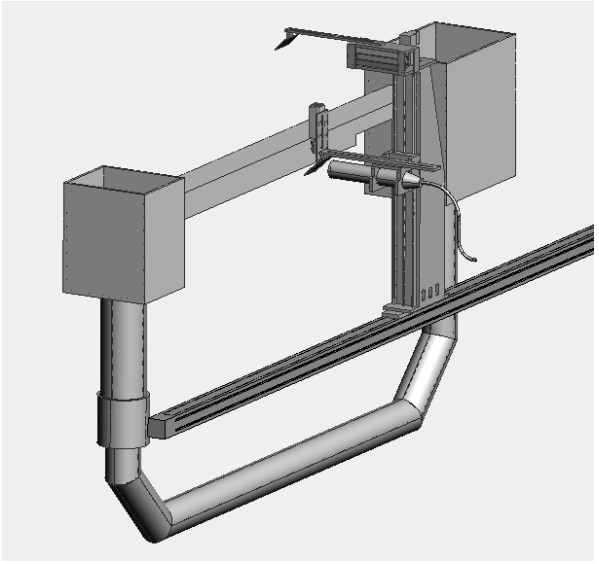

Fig. 1. Schematic of the test apparatus: water flows from right to left.

control computer based on the readings of the LDA. The LDA readings were fed into the control computer, which in turn, controlled the traverse acceleration.

The control code in the computer was designed for constant emulated-particle acceleration (LDA moves at constant acceleration). Since the traverse speed responds linearly to the input voltage, constant acceleration is achieved by updating the traverse velocity at 10 kHz. The desired acceleration is updated from the velocity measurements taken with the LDA. The speed of this loop is limited by the LDA data rate, but must happen faster than twice the Kolmogorov time scale to resolve all turbulent scales. In this particular flow, the Kolmogorov time scale is on the order of 5–20 ms (estimated through particle-image velocimetry (PIV) images and energy spectra data) and the largest time between data points is on the order of 5 ms, satisfying this constraint. In essence, we are performing a first-order forward difference approximation to the motion of the particle (traverse). We have tried some second-order schemes but all predictor–corrector schemes are hampered by the fact that we cannot get the fluid relative velocity at the next time step without moving the traverse and we cannot correct the traverse speed based on that new reading.

Finally, in order to estimate the local vorticity along the path of the particle, we mounted a moving PIV setup on the traverse as well. Using a red laser sheet to illuminate small seed in the water flow, we can optically filter the PIV information from the LDA information and get both fluid velocity and vorticity measurements. To do this, we used a color-separating dichroic filter at a 45 degree angle that reflects wavelengths above 600 nm and transmits wavelengths below. Since the lasers from the LDA are at 514 and 488 nm, they are transmitted through the filter. The laser sheet is at 670 nm and is therefore reflected off the filter to the camera. Hence the camera saw only light reflected from the laser sheet and not the LDA. The digital particle image velocimetry (DPIV) system (modeled after Willert and Gharib, 1991) consisted of a Lasiris 670 nm, 750 mW line generating diode laser and a Kodak ES 1 with a $1k \times 1k$ resolution (30 frames a second). By

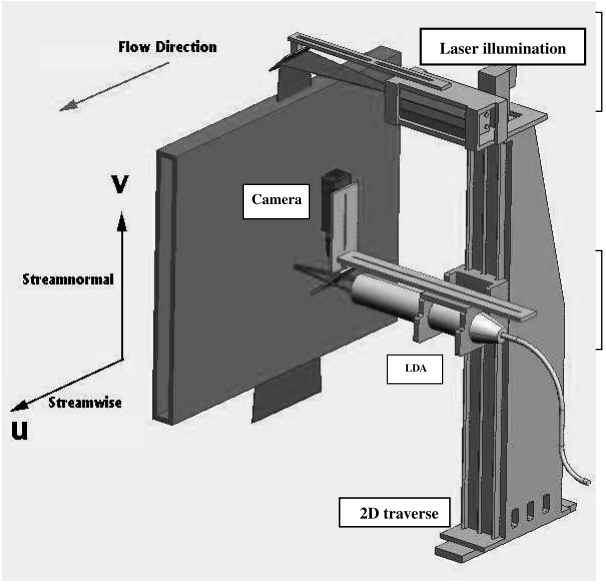

Fig. 2. Velocity feedback (LDA) and vorticity measurement (PIV) on the traverse.

pulsing the laser sheet for 5 ms, we could effectively freeze the flow and thereby get accurate fluid measurements. Fig. 2 shows the complete setup on the LDA and PIV systems on the traverse.

A 2% uncertainty for particle emulation was estimated based on traverse and LDA uncertainties. For the traverse system to accurately behave as a particle, it must respond to fluid fluctuations faster than the Kolmogorov time scale. To test the ability of the traverse to respond to sudden changes of the flow, we measured its response to a step input. Fig. 3 shows the traverse response time to be 5 ms. We can further test the overall setup by giving the traverse a sample voltage train and using the LDA to measure the traverse speed by measuring the speed of stationary water in the test section. Fig. 4 shows measured traverse velocities compared to desired velocity. An error less than 1% was found for both axes. The combined LDA uncertainty from the 11-bit A/D converter, the shift frequency and filter settings was less than 2% (Ainley, 1997).

The overall DPIV uncertainty was found to be 5% based on correlation correction and processing error. Spurious correlation points accounted for 7% of all vectors and were fixed by manually finding secondary correlation peaks or averaging the vector with its neighbors. We used a central difference algorithm to calculate local vorticity (McAndrew, 1998).

The experimental facility does have numerous limitations. First, the motion of the probe is limited to two dimensions. Adding a third component of velocity, while not computationally intensive, is experimentally difficult in that the three measuring volumes must remain coincident while the traverse is moving. This is easy to do in two dimensions but almost impossible in three (because of the change in index of refraction of the water and any curvature in the test section walls). Therefore we are really simulating a particle constrained to move in two dimensions while traveling through three-dimensional turbulence. Results from numerical simulations have shown (Ainley, 1997) that the particle behavior is not substantially different as long as there is little gradient in the fluid shear across this constrained plane – for instance, in the centerline of a

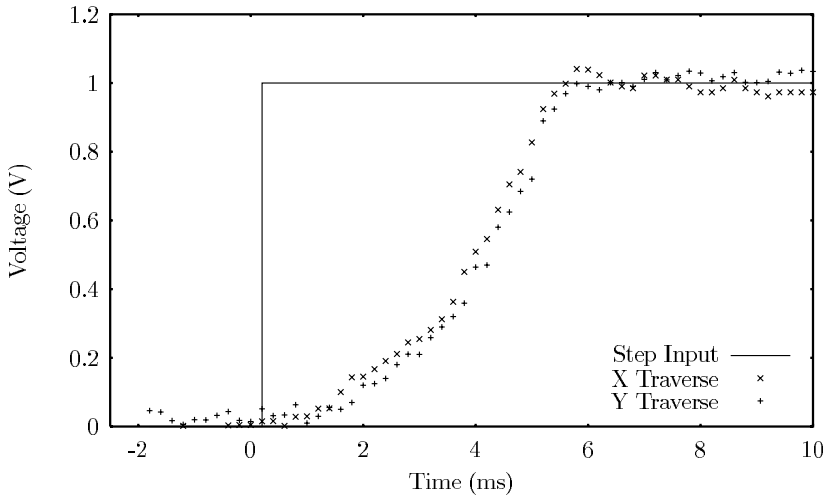

Fig. 3. The measured traverse response to step input in the desired velocity.

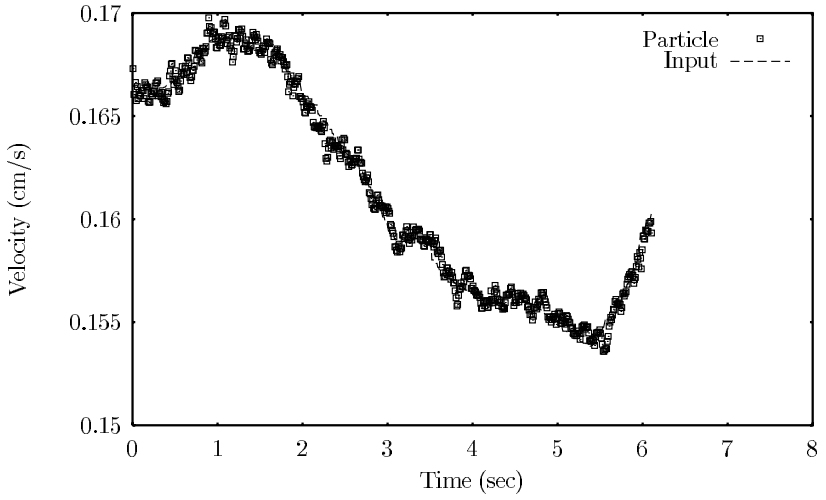

Fig. 4. Comparison of desired and measured traverse speed showing the ability of the traverse to follow the track.

channel. Second, in order to keep a small measuring volume, we have a step with a lower aspect ratio test section than desired. This geometrical constraint adds some three-dimensional effects to the fluid motion. Finally, since each run gives only a single measurement at a spatial location in the flow, to obtain statistically accurate data is time consuming, limiting the size of the measurable parameter space. The data presented were averages of 100 runs (or emulated particles).

The water flow (Reynolds number based on step height of 10,000) in the test section is indicative of most step flows. The inlet channel profile is within 5% of plug flow and the exit flow is fully developed. The reattachment point is seven step heights downstream of the step. Fig. 5(a) shows mean streamwise velocity distribution at 13 spatial locations in the test section, with a

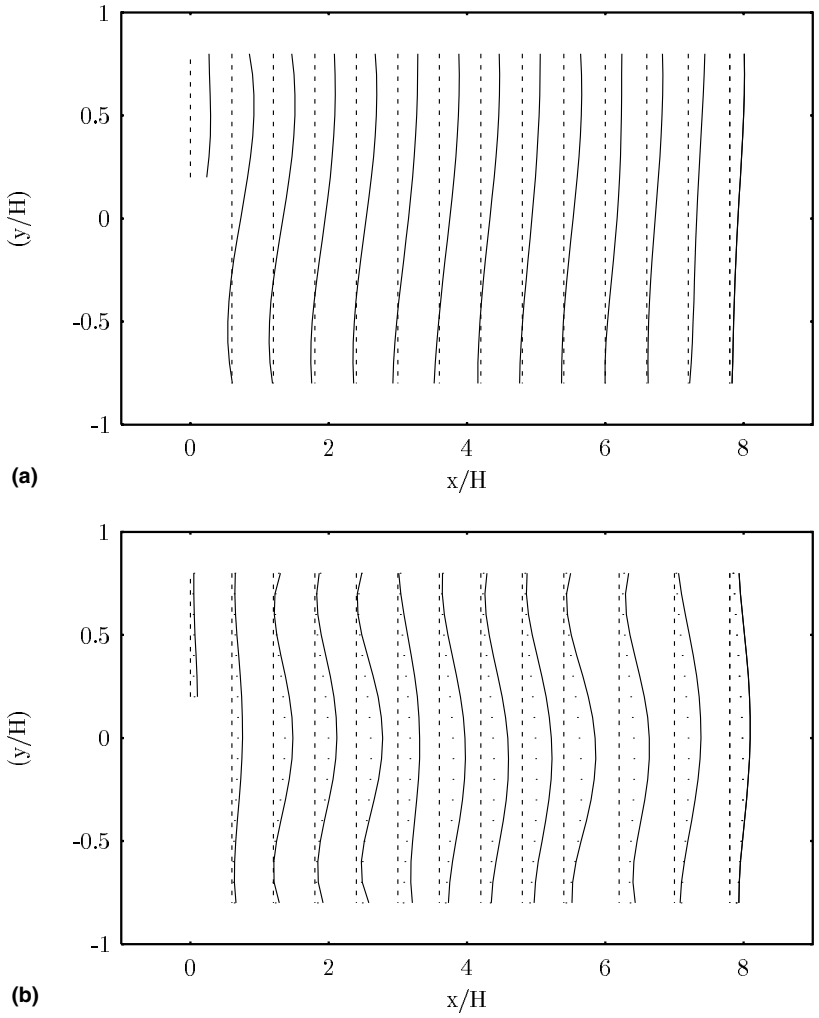

Fig. 5. (a) Mean Eulerian fluid velocity profiles at 13 downstream locations (centerline maximum at 0.2 m/s upstream of the step and 0.1 m/s downstream). (b) Fluid Eulerian turbulence intensity profiles at 13 downstream locations (peak intensities are 25% for the streamwise direction and 18% for the streamnormal direction).

maximum speed of 0.2 m/s upstream of the step and 0.1 m/s downstream. The dashed lines on the figure are lines of zero velocity for comparison. The turbulence intensity (the ratio of the rms velocity to the average inlet velocity) had a streamwise maximum of 25% (13% average) and a streamnormal maximum intensity of 18% (10% average) and is shown in Fig. 5(b). Both maxima occur in the shear layer behind the step. One can see the presence of the characteristic shear layer, reattachment point, and recirculating regions from these plots.

Three regions of turbulence characterized the channel: the free stream, the shear layer, and the recirculating region. The free stream turbulence has an integral time scale (T), calculated by the area under the fluid velocity autocorrelation, of 0.1 s upstream of the step and 0.2 s after reattachment. The non-dimensional time is defined as

$$\hat{T} = \frac{TU_{\text{inlet}}}{H} \tag{2}$$

(again H is the step height) and has the value of 0.4 upstream of the step and 0.8 downstream of reattachment. The shear layer, or the region between the free stream and the recirculation region, has an integral time scale of 0.07 s ($\hat{T} = 0.28$) while in the recirculation region, it is similar to the flow after reattachment at 0.2 s or $\hat{T} = 0.8$. The shear layer has a much smaller integral time scale because it is the region where the fluid is mixing between the free stream and the recirculation region. The minimum Kolmogorov time scale was estimated to be 5 ms from PIV images and energy spectra data. These estimates were made from the PIV images using a central differencing scheme to estimate the dissipation. From this, one can estimate the Kolmogorov time scale.

3. Results

Given the inhomogeneity of the flow, the data from the backward-facing step flow are inherently more confusing than homogeneous channel flow. The shear layer and recirculation region split the channel into regions where the particle behaves differently and must be accounted for in data reduction. That is, an emulated particle that remains in the recirculation region throughout its run will have seen different turbulence from a particle that crossed the shear layer while a particle that remains in the free stream will behave more closely to a particle in a homogeneous turbulent channel flow. Simple homogeneous flow was investigated by Ainley (1997). This article looks at bulk behaviors in inhomogeneous turbulence. Detailed measurement in both channels will be the next undertaking.

Once the flow behavior in the test section was established, the next step was to take measurements along the path of the emulated particle. Fig. 6 shows two sample comparisons of the particle and surrounding fluid velocities. Fig. 6(a) is a sluggish particle and Fig. 6(b) shows a particle with a response time on the order of the fluid time scale. Typically, one would compare the fluid to particle time scales through the Stokes number (the ratio of the two), but since the turbulence scales change along the path of the particle as it goes in and out of the shear layer, we choose to cite only the particle response time. All measurements had the emulated particle starting 1.4 step heights upstream of the step and in the middle of the channel. Note that the particle in Fig. 6(a) reacts to little of the fluid fluctuation whereas the one in Fig. 6(b) follows all but the highest frequency fluctuation. Both of these particles stayed in the freestream flow, never entering the recirculating region or the shear layer. This is more apparent in the average particle streamnormal velocity fluctuation (Fig. 7). Smaller particles are more affected by the turbulence and therefore have a higher fluctuating velocity component.

The turbulence in the backward-facing step was maintained at a constant Reynolds number during all experiments, so average fluid fluctuating velocities should yield similar results irrespective of the particle time constant if the particles are randomly sampling the surrounding turbulence. Fig. 8 shows the measured fluid fluctuations in the streamnormal direction versus distance downstream. Again, these are only the subset of particles which were started 1.4 step heights upstream of the step and stayed in the free stream of the channel throughout their runs. Note that all the particles do not see the same fluid turbulence. Heavier particles are seeing a higher amount of fluid fluctuation. This is because they are less likely to follow the fluid motions

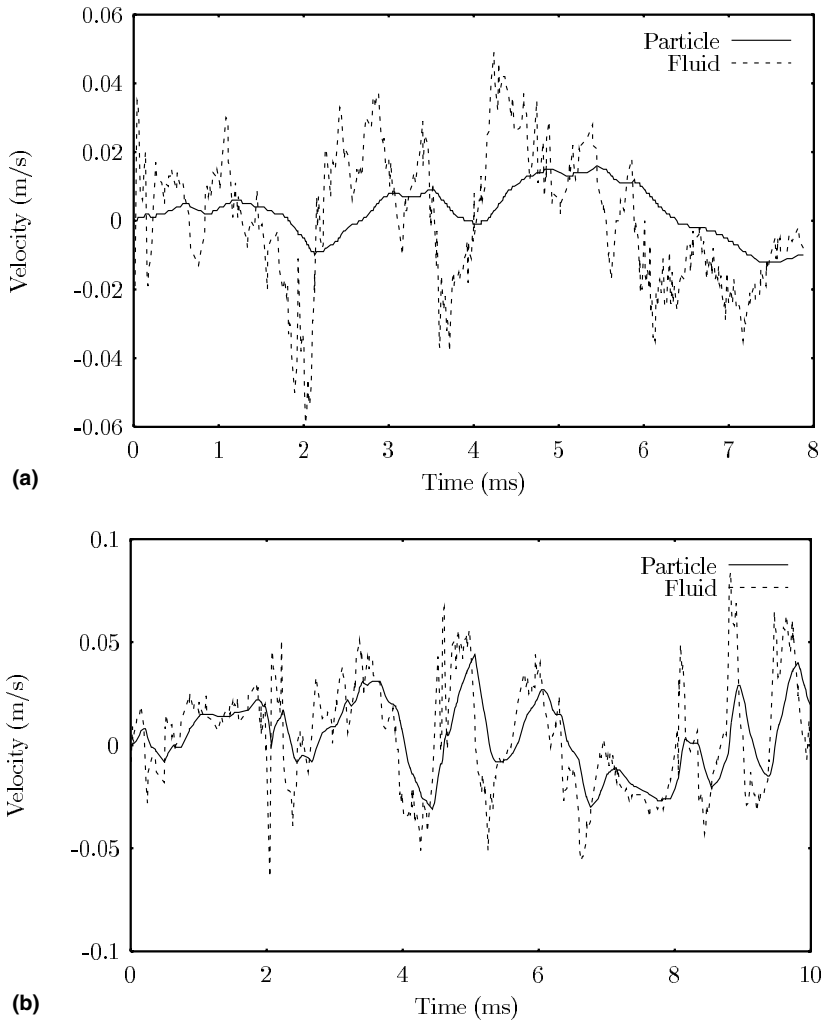

Fig. 6. (a) Particle and fluid velocity ($\tau_p = 1$ s). (b) Particle and fluid velocity ($\tau_p = 200$ ms).

as quickly as their smaller time constant counterparts. Therefore in vortical regions, these particles will have a larger instantaneous slip velocity, leading to a higher perceived fluid turbulence. Further, smaller time constant particles will tend to preferentially concentrate in the regions of lower vorticity and therefore not see the greater fluid fluctuations. Fig. 9 shows an example fluid velocity autocorrelation along the path of the emulated particle. One can see both the continuity effect and the non-isotropy of the shear layer clearly.

Since we simulate the particle motion, we can look at particle trajectories. Fig. 10 shows one sample trajectory as the emulated particle (LDA measuring volume) gets flung out of the recirculation region. Particle dispersion or mean-square displacement was calculated for varying particle time constants. For a particle in the backward-facing step, the fluid characteristics change depending on the location of the particle in the channel geometry. When a particle remains in the

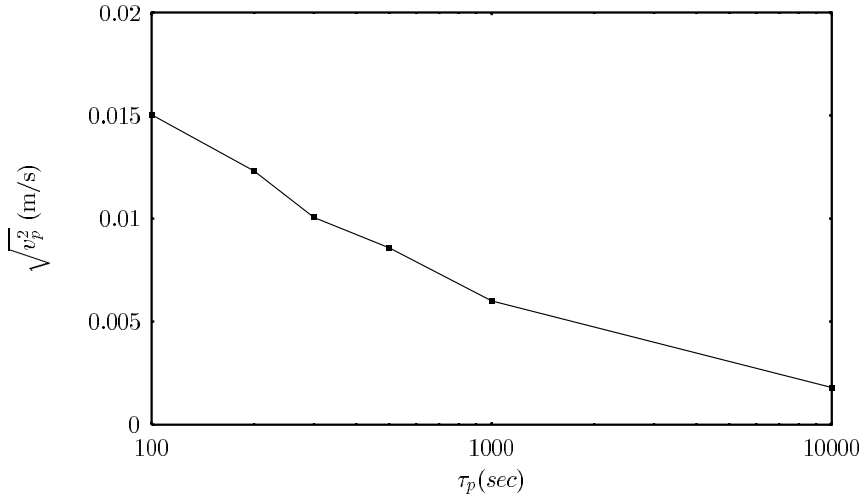

Fig. 7. Particle streamnormal velocity fluctuation as a function of time constant.

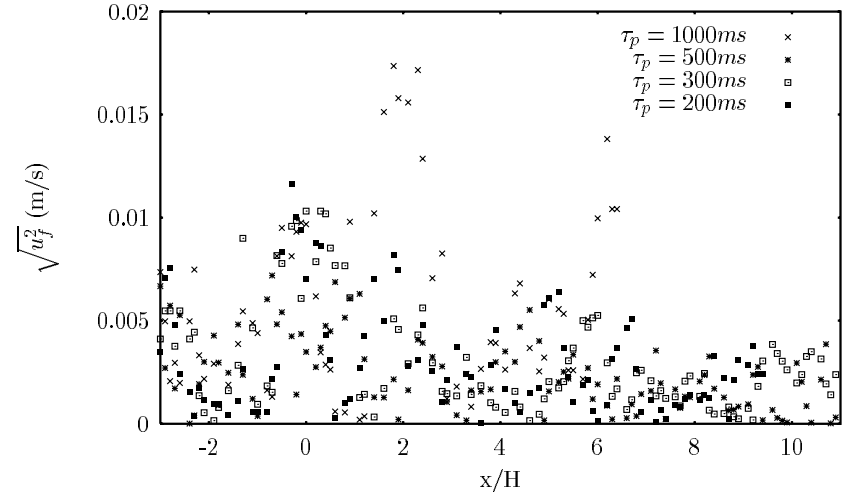

Fig. 8. Average fluid turbulence along the particle path.

freestream, the channel turbulence does not vary as much as a particle moving through the shear layer. By starting emulated particles at the same upstream location and examining only those that remain in the free stream throughout their run, dispersion data has similar trends to homogeneous turbulence but has the inhomogeneity of the expansion.

Fig. 11 shows the expected trend of particle dispersion increasing with decreasing particle time constant. Particle trajectories that entered the shear layer had substantially different mean square displacements that varied depending on when the particle entered and exited the shear layer. This is clearly seen in Fig. 12 that shows particle dispersion data for a 100 ms particle originating in the recirculation region (three step heights downstream of the step and 0.5 step heights from the

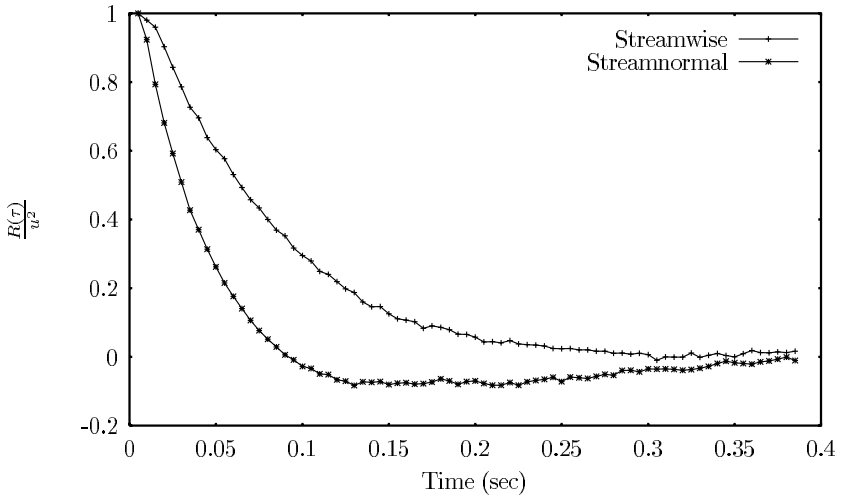

Fig. 9. Sample fluid velocity autocorrelation in the shear layer.

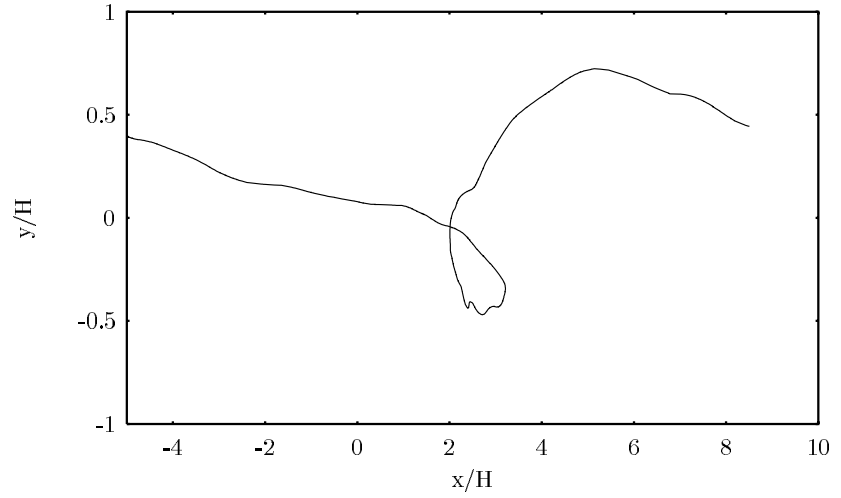

Fig. 10. Sample particle trajectory in the shear layer.

bottom) compared to free stream particle dispersion. Particles that remained in the recirculation region dispersed 25% more than free stream particles. Dispersion increased with the number of shear layer crossings. Particles that left the recirculation region dispersed 50% more than particles that remained in the free stream throughout their run. The data are plotted versus time because the particles are not transported similar lengths downstream. Note that there were no particles that crossed the shear layer more than twice. One can add full numerical simulations to gain more insight on the effects of fluid structures (Coppen et al., 2001).

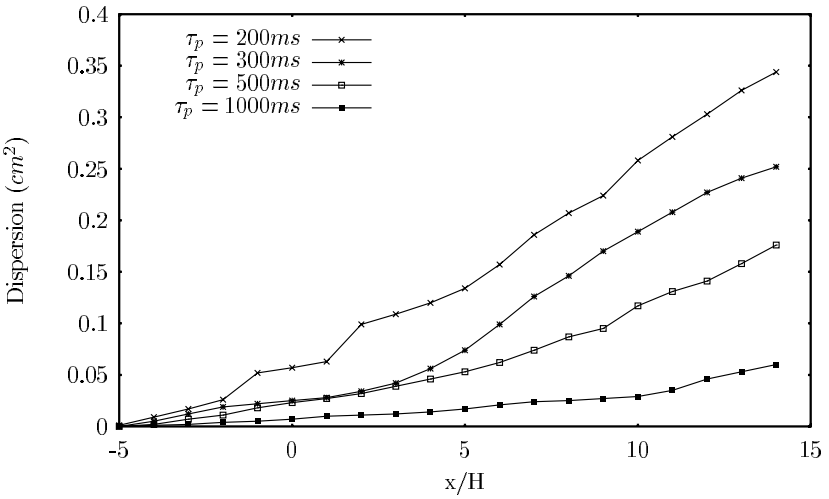

Fig. 11. Mean square particle dispersion for varying time constants.

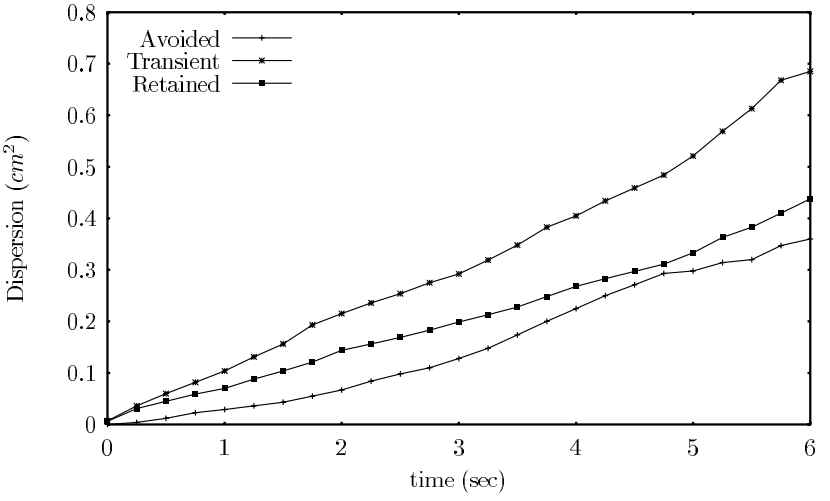

Fig. 12. The effect of crossing the shear layer on particle dispersion.

Further, one can examine the range of particle velocities at a given spatial location in the flow. Fig. 13 shows the distribution of particle velocities (normalized by the number of occurrences of the most common velocity) at three spatial locations in the flow for two different particle sizes. Fig. 13(a) shows the distribution for the 100 ms particles upstream of the step, in the recirculation region, and downstream of the step. These distributions were found by extracting all of the particle velocities that were measured in a box two step heights long ($2H$) and half a step height tall ($0.5H$). One can see that the particle distribution in the recirculation region is much larger than outside, where their velocity distributions are roughly equal. The measurements for inside the recirculation region were for particles moving in a box $0.5H \times 0.5H$. This is most likely a

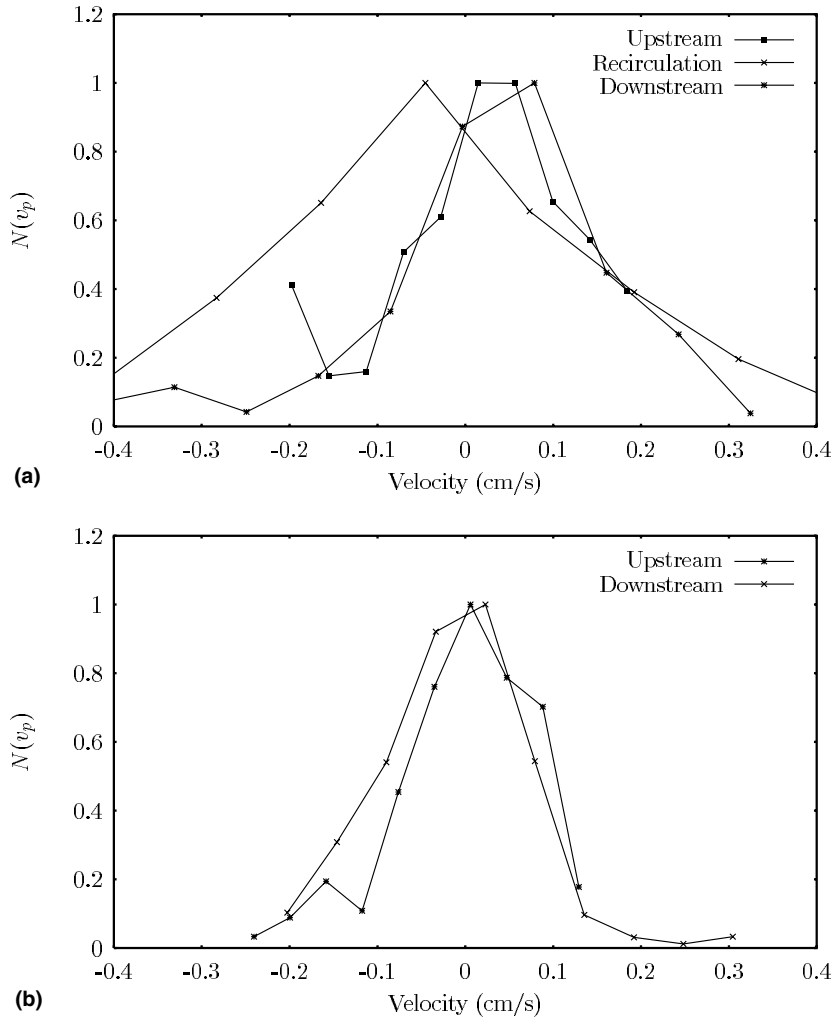

Fig. 13. (a) Normalized particle velocity pdf at three spatial locations in the flow ($\tau_p = 100$ ms). (b) Normalized particle velocity pdf at two spatial locations in the flow ($\tau_p = 500$ ms).

result of the varying velocity histories of the different particles. Also note the increase in the variation in particle velocities in the recirculation region. As one would expect, the variance in the particle velocity decreases for the larger time constant particles (Fig. 13(b)) since the particles are losing their ability to respond to fluid fluctuations. We were unable to make a similar measurement in the recirculation region as the heavy particles would either move toward the walls or bounce out of the region.

Finally, one can also look at the vorticity along the path of the particle to correlate fluid structures to particle motions. The local fluid vorticity measurements were estimated from DPIV data taken during the motion of the traverse. The uncertainty in these measurements is rather large due to the limited laser power of the light sheet. Further, we can only measure one

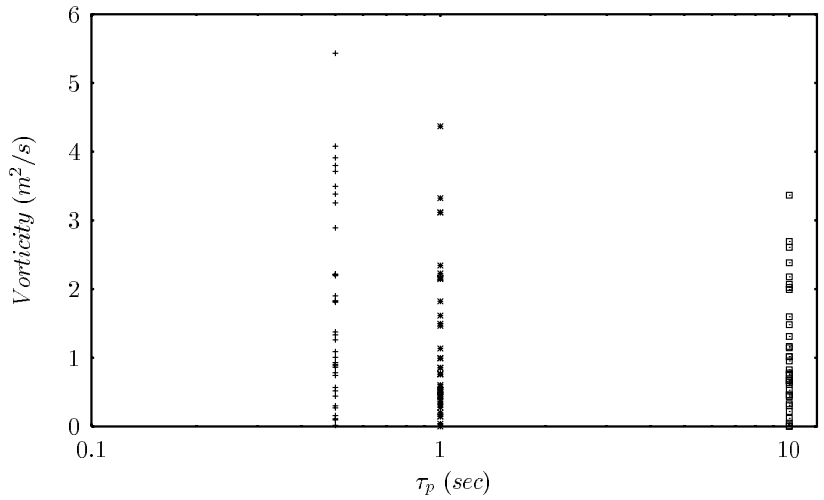

Fig. 14. Measured streamnormal vorticity along the path of a particle for different particle time constants.

component of vorticity and therefore are seeing only a part of the picture. Fig. 14 shows the range of fluid vorticity seen by different particles. The results show the particles taking a path of least vorticity. That is, the largest time constant particles are getting flung out of the vortical regions, preferring to stay in the straining regions. The lighter particles are thrown less, and therefore sample more of the vorticity of the surrounding flow. This has been seen in previous simulations as well. One can then try to correlate the local particle acceleration with the local fluid vorticity, but the limitations of only one component of vorticity and the large uncertainty in the measurements reduce the effects of any trends. The only apparent trend shows that lighter particles are subject to larger accelerations and higher vorticity.

4. Conclusion

The presented quasi-numerical investigation of a particle-laden flow has been shown to be a useful technique; it examines a larger range of turbulent scales than full numerical simulation while providing data in the particle-Lagrangian reference frame, currently impossible with experimental work. Previous work was conducted (1997) to study homogeneous flow in a turbulent channel. In this article, average fluid and particle statistics, including local fluid vorticity, were shown for a single Reynolds number flow in a backward-facing step. The greatest difficulty in modeling the measured results is in deciding how to take into account the motion of the particles in and out of the shear layer. Interaction with the shear layer increases the range of turbulence seen by the particle and therefore the fluid will have more of an effect on the particle motion than on the particle that never entered the shear layer. Future work will be aimed at making conditionally averaged measurements of fluid and particle velocities, looking only at particles that pass through various sections of the shear layer. Additionally, results will be compared to LES results and more channel data will be added.

Acknowledgements

The authors would like to thank the NSF for funding the work and acknowledge the help of many other students at Tufts University who helped in making the measurements.

References

Ainley, S.B., 1997. Measuring Particle Response to Fluid Turbulence in the Particle-Lagrangian Reference Frame. Ph.D. thesis, Tufts University.

Ainley, S.B., Rogers, C.B., Eaton, J.K., 1997. A technique for fluid velocity measurements in the particle-Lagrangian reference frame. In: Proceedings of the Seventh International Symposium on Gas-particle Flows, FEDSM97-3570, Vancouver, BC.

Armaly, B.F., Durst, F., Pereira, J.C.F., Schonung, B., 1983. Experimental and theoretical investigation of backward-facing step flow. J. Fluid Mech. 127, 473–496.

Berlemont, A., Desjonqueres, P., Gouesbet, G., 1990. Particle Lagrangian simulation in turbulent flows. Int. J. Multiphase Flows 16, 19–34.

Coppen, S.W., Manno, V., Rogers, C.B., 2001. Turbulence characteristics along the path of a heavy particle. J. Comput. Fluids 30, 257–270.

Coppen, S.W., McAndrew, D., Rogers, C.B., 1999. Correlating Particle Dynamics with Local Fluid Structures in Turbulent Flows. ASME FEDSM99-7894, San Francisco, CA.

Eaton, J.K., Fessler, J.R., 1994. Preferential concentration of particles by turbulence. Int. J. Multiphase Flow. 20 (Suppl.) 169–209.

Elghobashi, S.E., Truesdell, G.C., 1992. Direct simulation of particle dispersion in a decaying isotropic turbulence. J. Fluid Mech. 242, 655–700.

Kiger, K.T., Lasheras, J.C., 1997. Dissipation due to particle/turbulence interaction in a two-phase, turbulent, shear layer. Phys. Fluids 9, 3005–3023.

Le, H., Moin, P., Kim, J., 1997. Direct numerical simulation of turbulent flow over a backward-facing step. J. Fluid Mech. 330, 349–374.

Longmire, E.K., Eaton, J.K., 1992. Structure of a particle-laden round jet. J. Fluid Mech. 236, 217–257.

Maxey, M.R., Riley, J.J., 1983. Equation of motion for a small rigid sphere in a nonuniform flow. Phys. Fluids 26, 883–889.

McAndrew, D., 1998. Measurements of Fluid Turbulence Along the Path of a Heavy Particle in a Backward-Facing Step Flow. Master's Thesis, Tufts University, Medford, MA.

Rouson, D.W., Eaton, J.K., Abrahamson, S.D., 1997. A Direct Numerical Simulation of a Particle-Laden Turbulent Channel Flow. Report TSD-101, Stanford University.

Rogers, C.B., Eaton, J.K., 1990. The behavior of solid particles in a vertical turbulent boundary layer in air. Int. J. Multiphase Flow 16, 819–834.

Ruck, B., Makiola, B., 1988. Particle dispersion in a single-sided backward-facing step flow. Int. J. Multiphase Flow 14, 787–800.

Simonin, O., Deutsch, E., Minier, J.P., 1993. Eulerian prediction of the fluid/particle correlated motion of turbulent two-phase flows. Appl. Sci. Res. 51, 275–283.

Snyder, W.H., Lumley, J.L., 1971. Some measurements of particle velocity autocorrelation functions in a turbulent flow. J. Fluid Mech. 48, 41–71.

Squires, K.D., Eaton, J.K., 1991a. Lagrangian and Eulerain statistics obtained from direct numerical simulations of homogenous turbulence. Phys. Fluids A 3, 130–143.

Squires, K.D., Eaton, J.K., 1991b. Measurements of particle dispersion obtained from direct numerical simulations of isotropic turbulence. J. Fluid Mech. 226, 1–35.

Tchen, C.M., 1947. Mean Value and Correlation Problems Connected with the Motion of Small Particles Suspended in a Turbulent Fluid. Ph.D. thesis, Martinus Nijhoff, Delft, The Hague.

Wells, A.C., Stock, D.E., 1983. The effect of crossing trajectories on the dispersion of particles in a turbulent flow. J. Fluid Mech. 105, 487–505.
Willert, C.E., Gharib, M., 1991. Digital particle image velocimetry. Exp. Fluids 10, 181–193.
Yudine, M.I., 1959. Physical considerations on heavy particle diffusion. Adv. Geophys. 6, 185–191.